3. Quantum Glassy Dynamics in world-record 26% Si PV

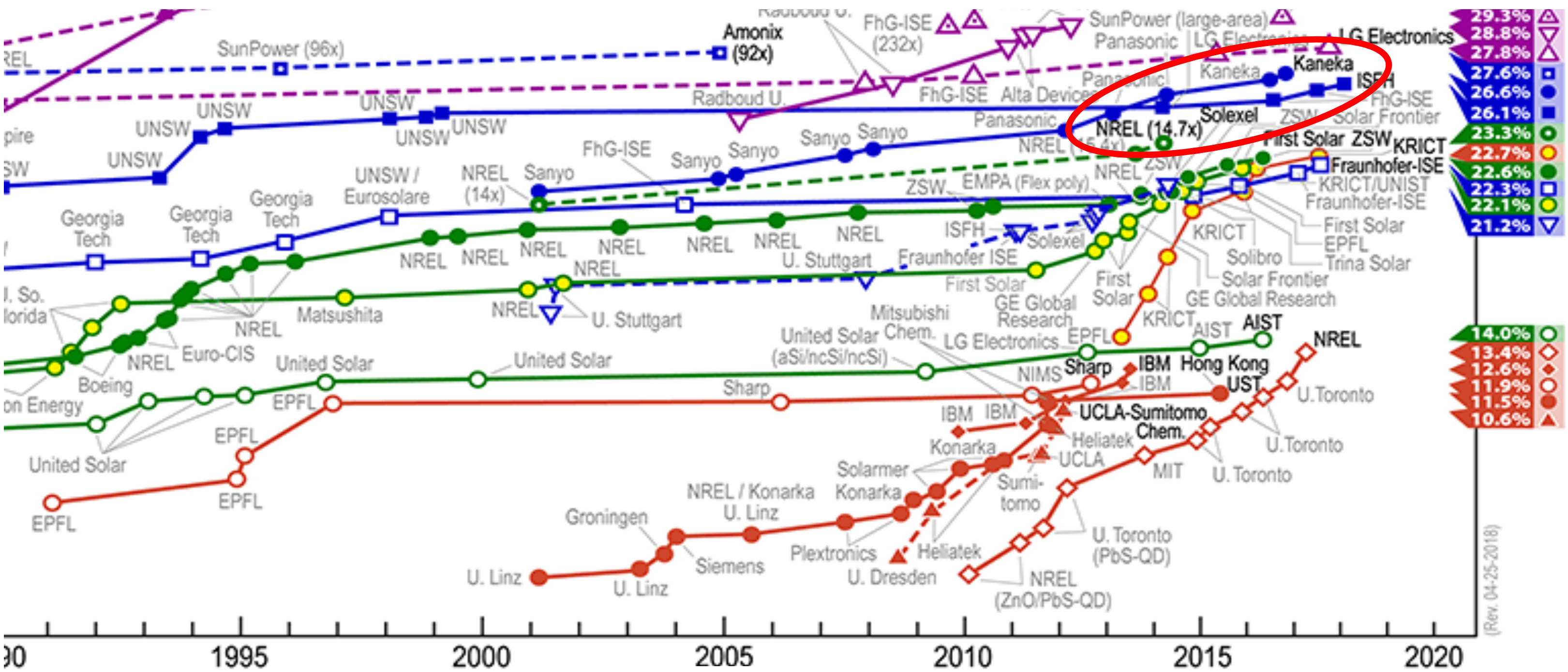

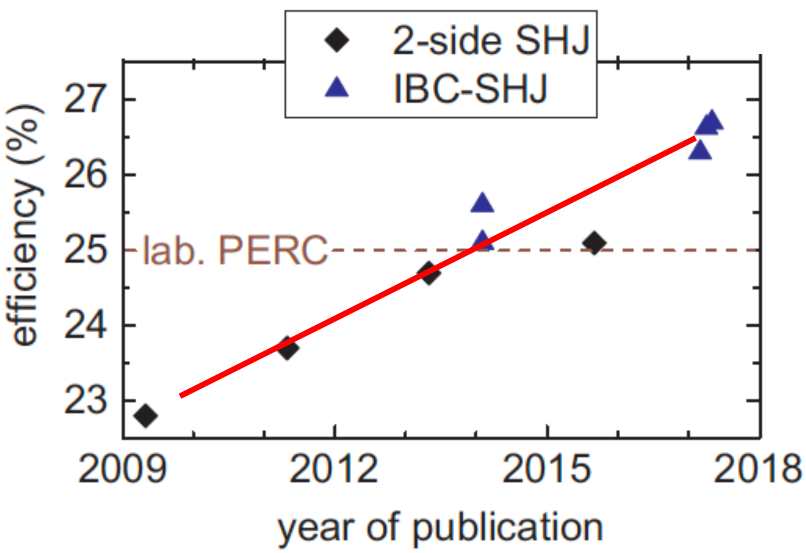

In spite of rapid rise in efficiency and the world record, SHJ (HIT) Si PV cells are not accepted by the market. Why?

Light-induced defect generation drives performance degradation, delays market entry of world-record HIT Si PV

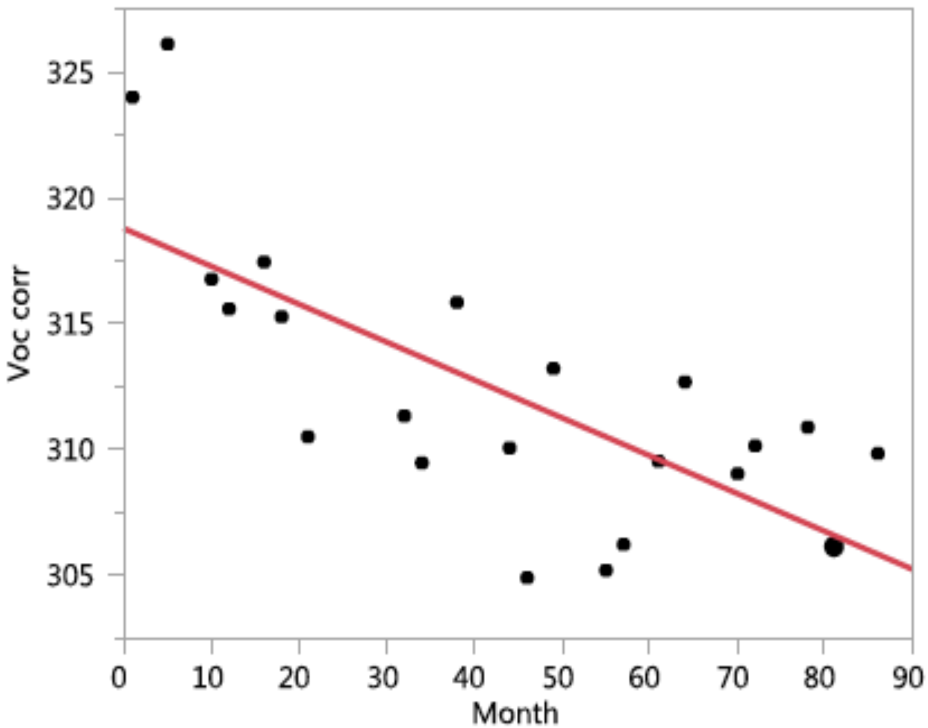

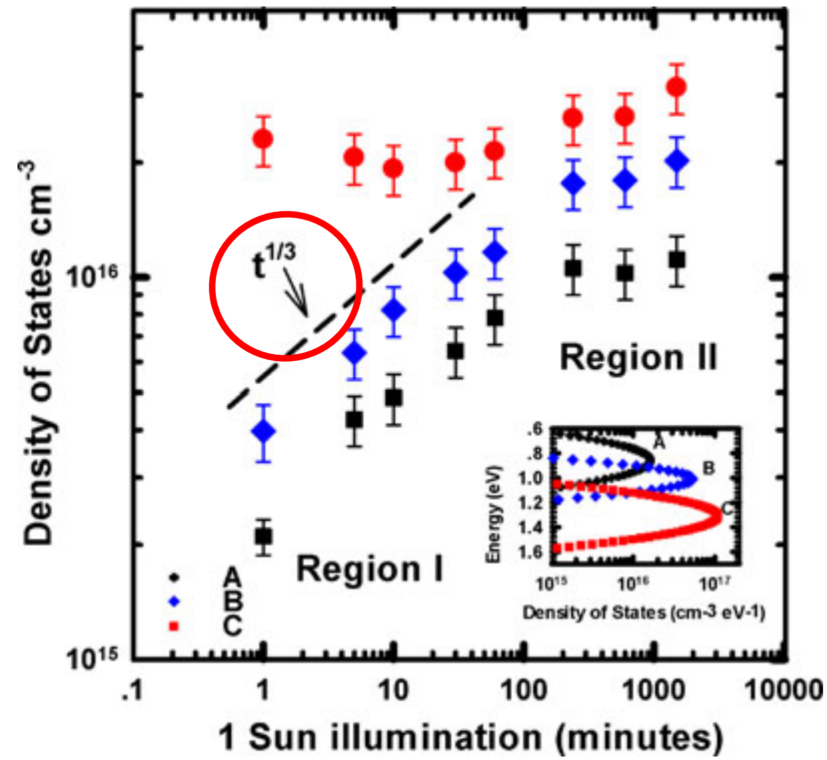

New degradation channel: Voc
Jordan-Johnston NREL 2018

Stabler-Wronskii: slow generation of light-induced defects:
$t^{1/3}$: collective/glassy dynamics?

Hydrogen escapes Si (di-)vacancies, leaves behind dangling bonds that act as recombination defects for PV

Si Divacancy

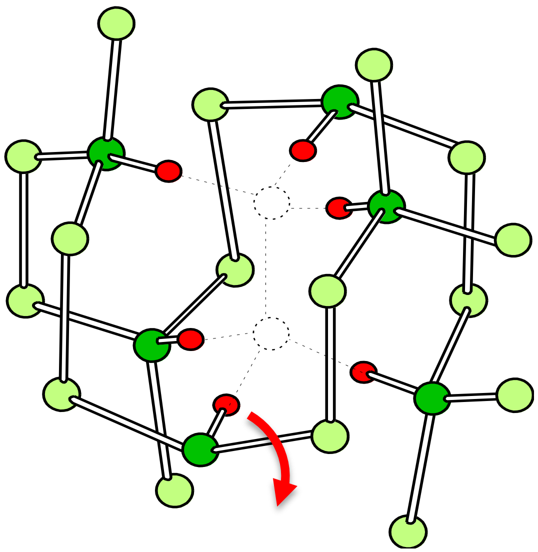

H escaping divacancy across barrier

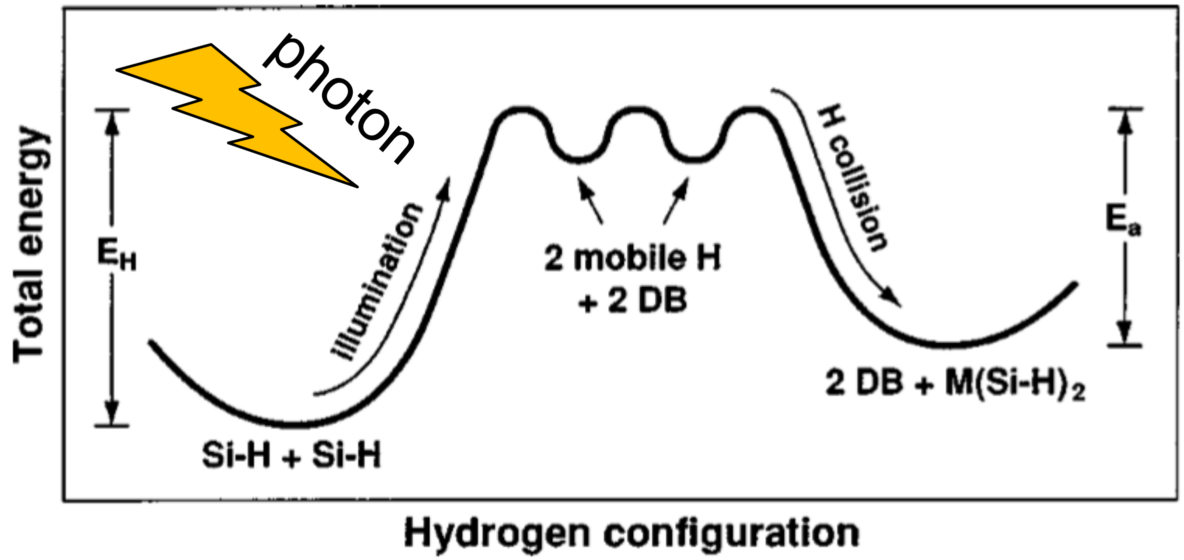

Defect Dynamics

Photon absorption creates dangling bond and H inside (di-)vacancy

H escapes vacancy across barrier, becomes mobile

Mobile H propagates across disordered energy landscape of a-Si

Mobile H eventually recombines with a dangling bond, reduces defect density

Model defected, hydrogenated a-Si absorber

Determine energy barriers that control H escape and thus dangling bond formation, and their distribution

From energy barrier distribution, determine distribution of timescales, and time dependent defect density $n_{def}(t)$

Determine how the defect density $n_{def}(t)$ controls Voc(t):

(1) Kinetic Monte Carlo simulation

(2) analytic calculation

Structure: CHASSM; Barriers: LAMMPS

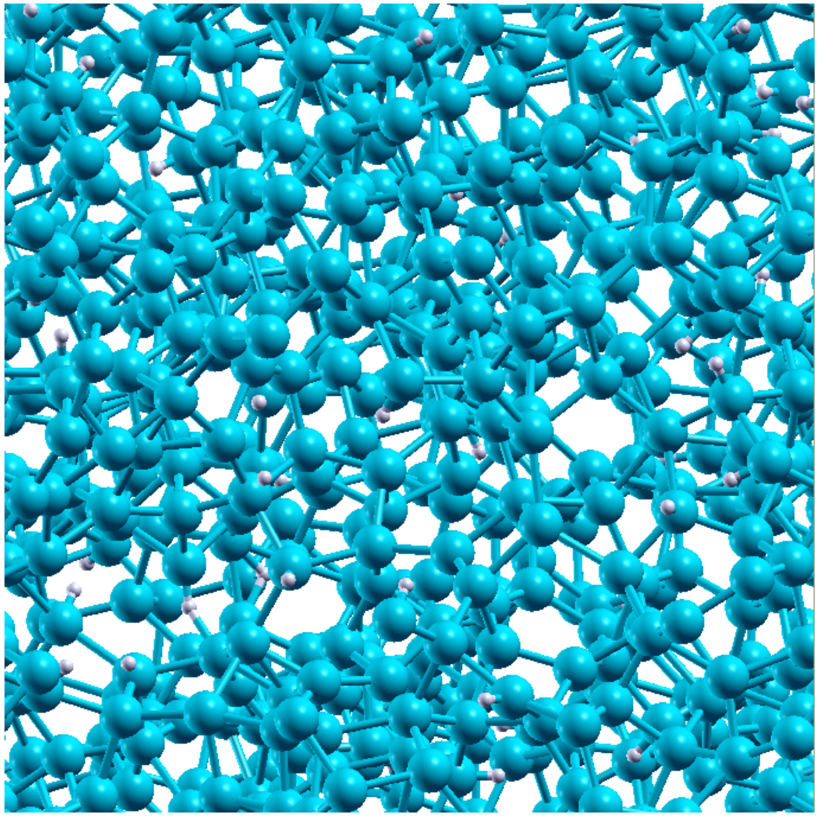

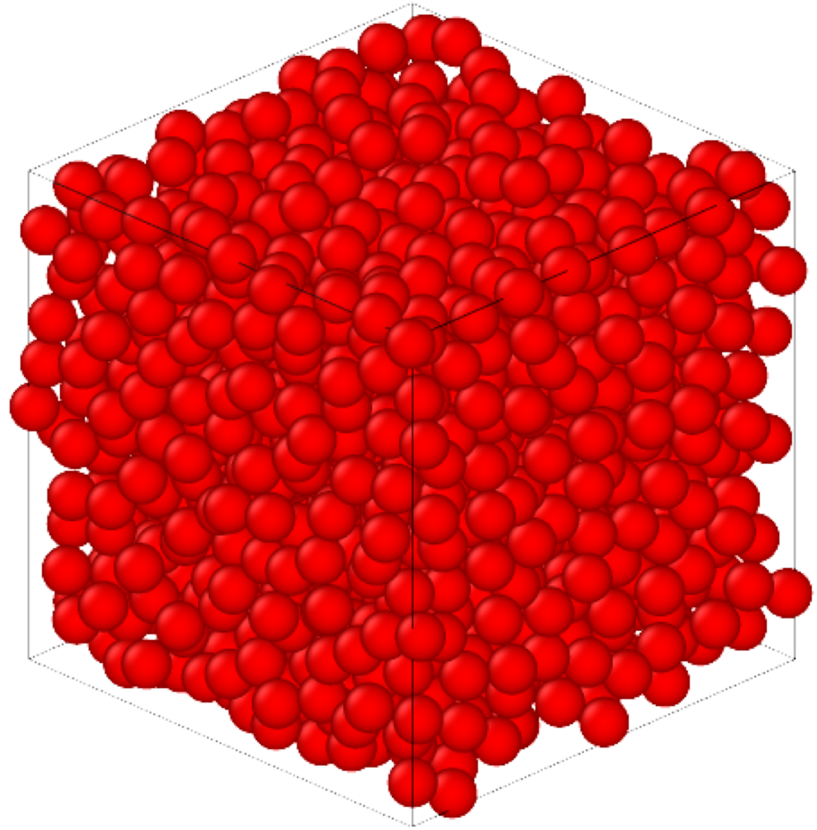

Best structure generator: CHASSM (Computational Hydrogenated Amorphous Structure Maker) code, developed at MIT.

Based on WWW code, developed at UC Davis

More agile code: LAMMPS, can model atom dynamics

Barrier determination: Nudged Elastic Band

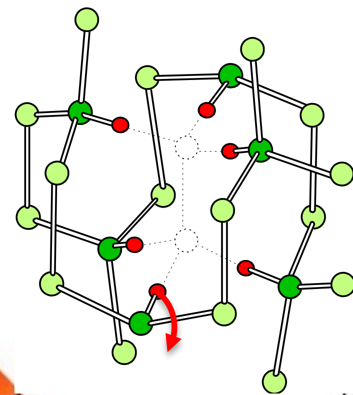

Distribution of Barriers $P(E_{barrier})$
Distribution of Escape times τ:
$P(\tau) \sim P(t_0 \exp(E_{barrier}/kT))$

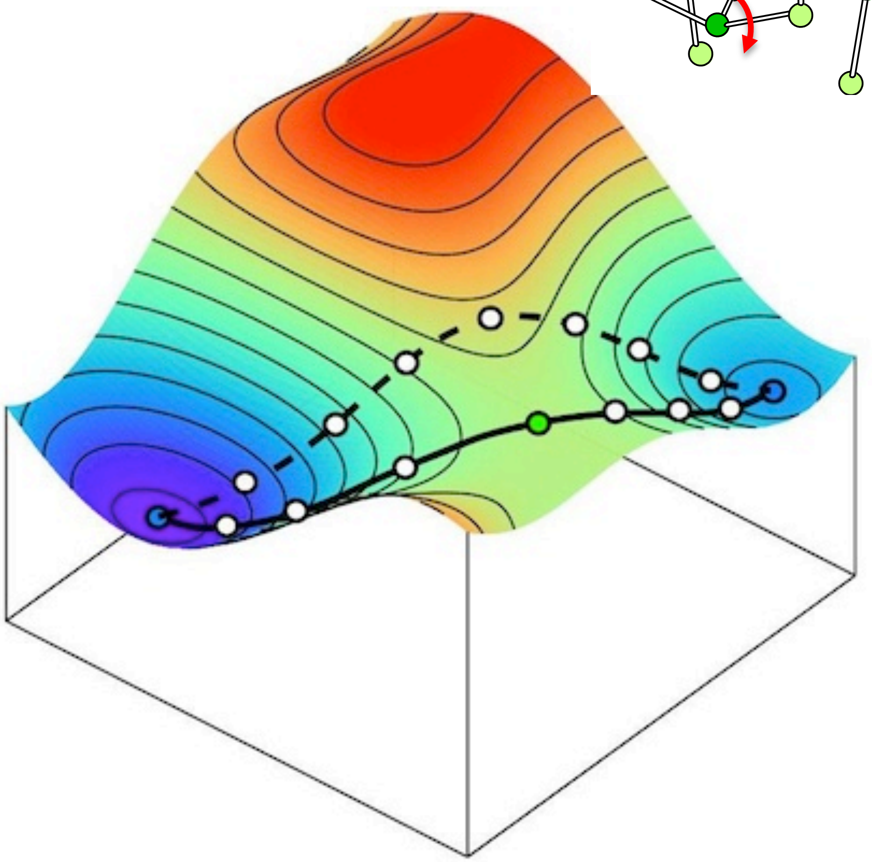

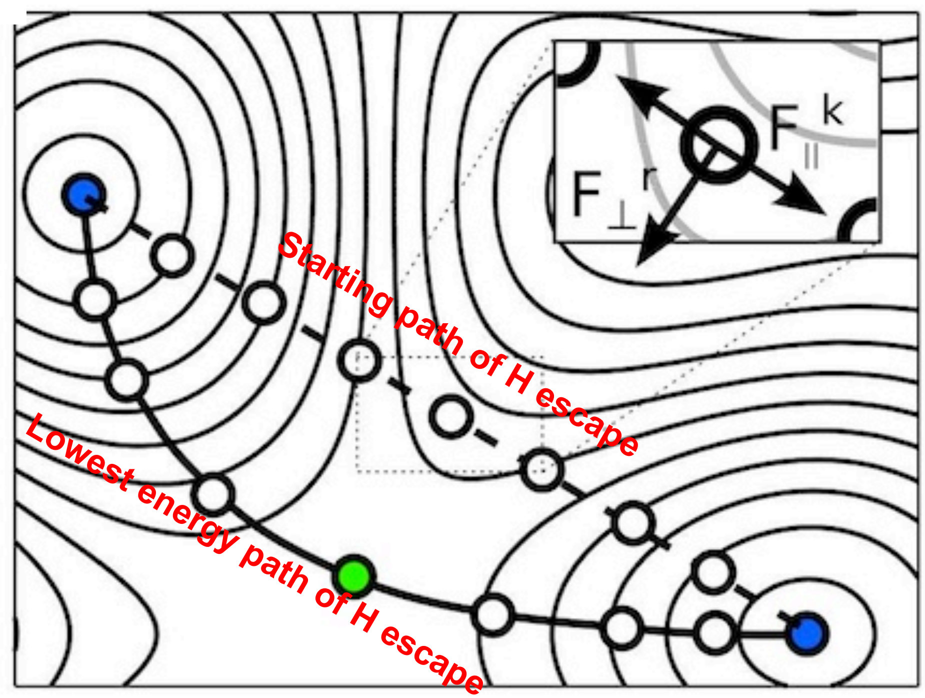

Barrier = E(green)-E(blue)

Locating defects, capturing escape times

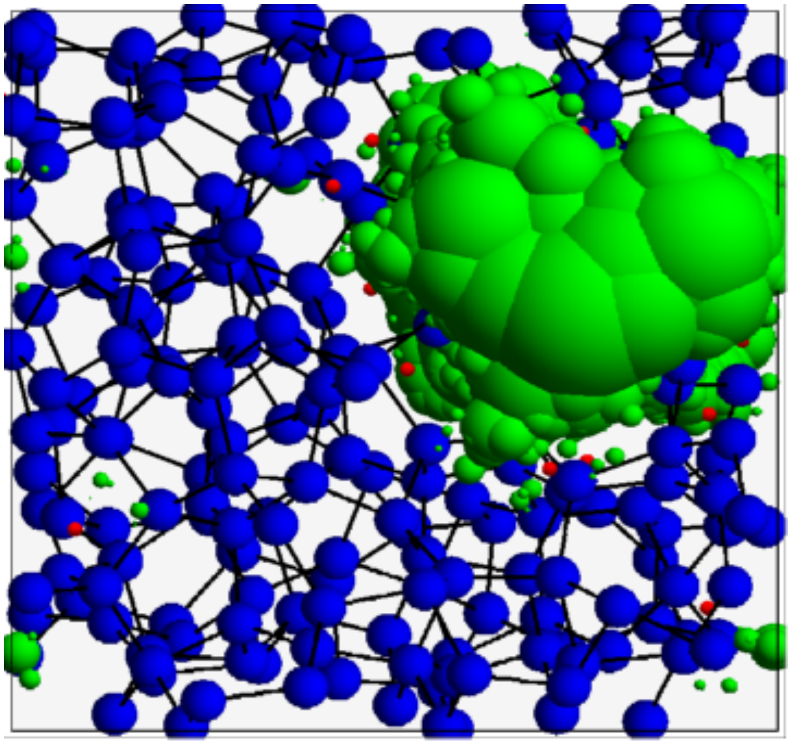

Void (green) in a-Si:H
with density 1.91 g/cm^3

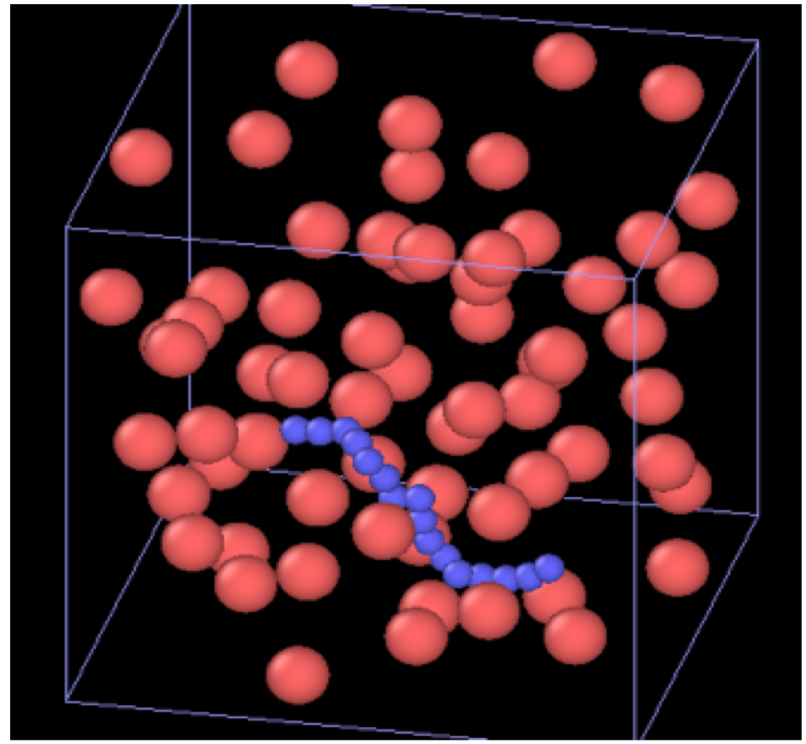

Escape path, found by
Nudged Elastic Band

Escape time statistics, spans 8 decades

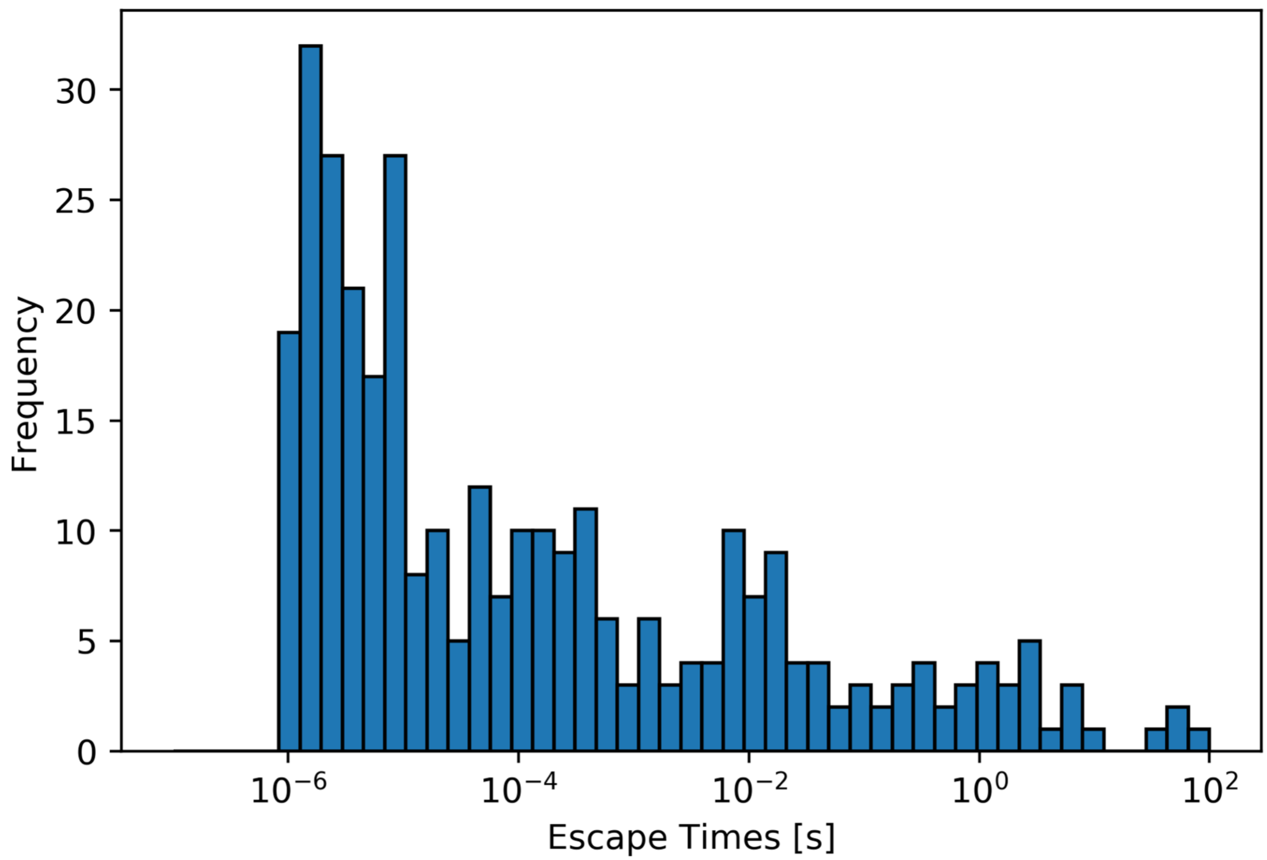

Impact of defect density $n_{def}(t)$ on Voc

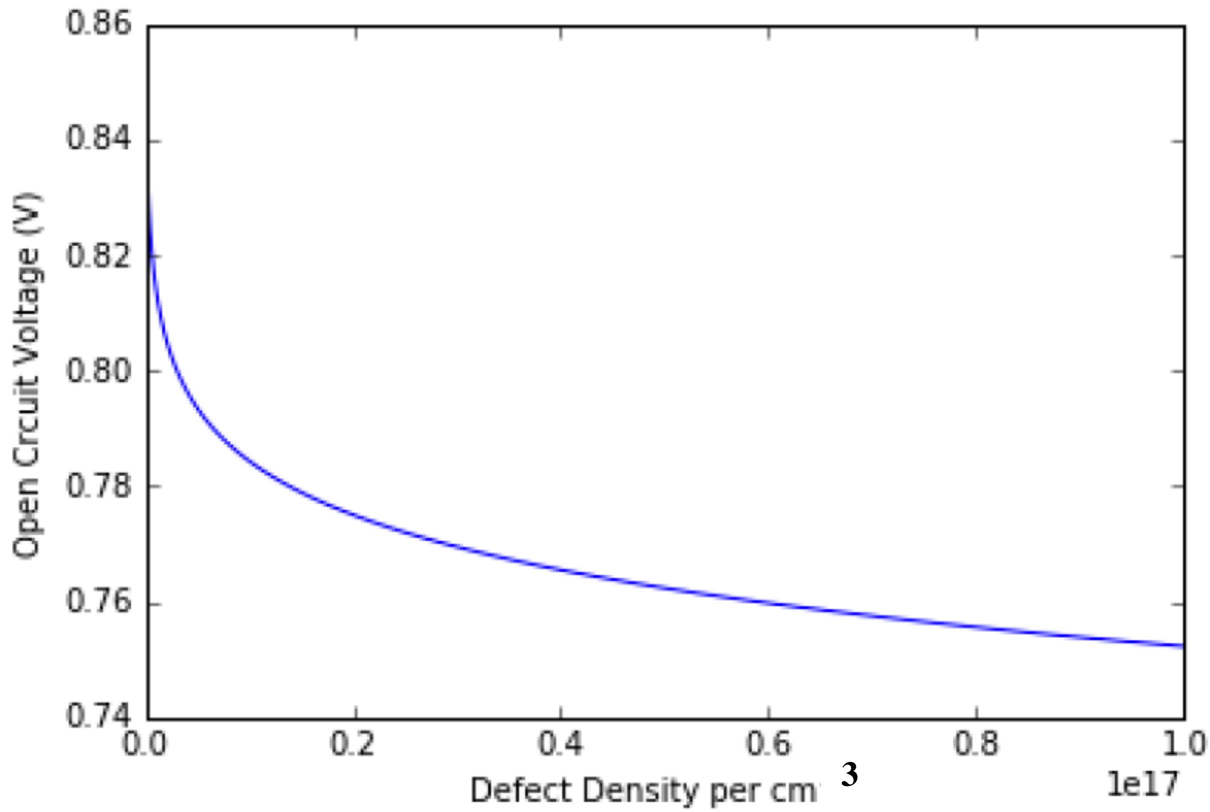

This curve translates the defect density $n_{def}(t)$ into a time dependent Voc degradation

Slow defect generation, control defect density to make HIT Si PV reliable

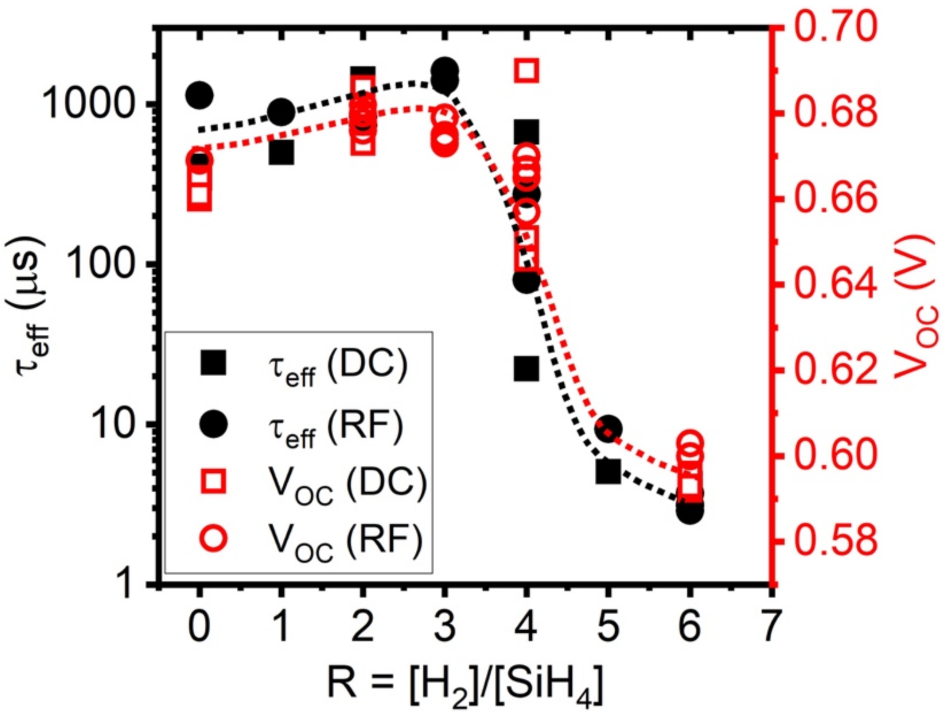

Effective lifetime (black) and V_{OC} (red) for a-Si/c-Si HJ solar cells deposited by RF or DC plasma for different H dilution ratios R_H.

Note steep edge at R_H = 4.
V_{oc} imroved by 50 mV.

4. Renormalization Group helps Permanent Magnet Development for Toyota Prius

Rare earth elements are rare

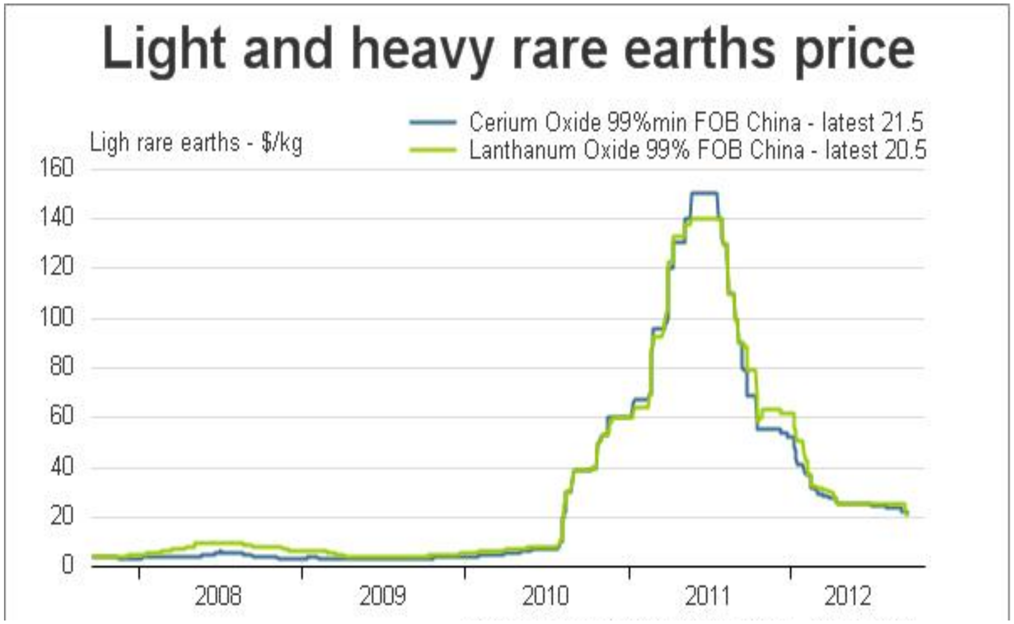

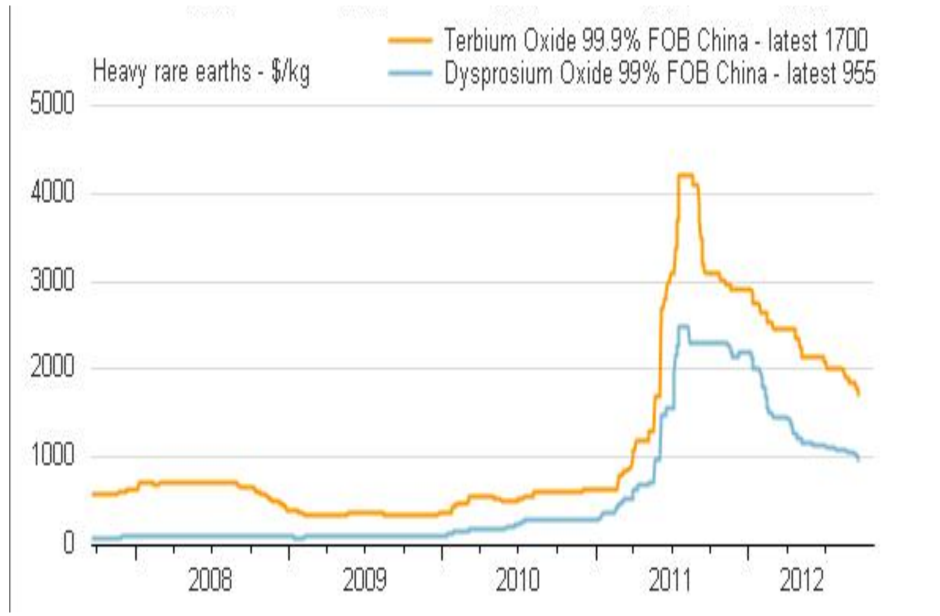

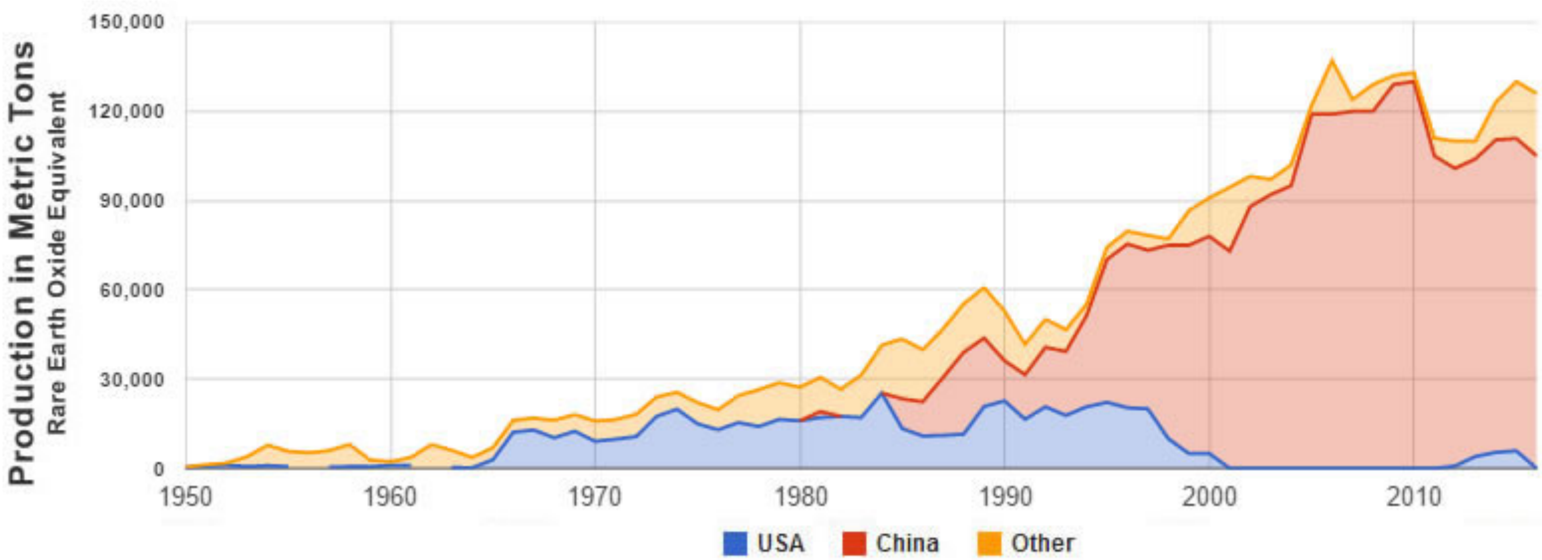

Hierarchical simulation of reversal in permanent magnets

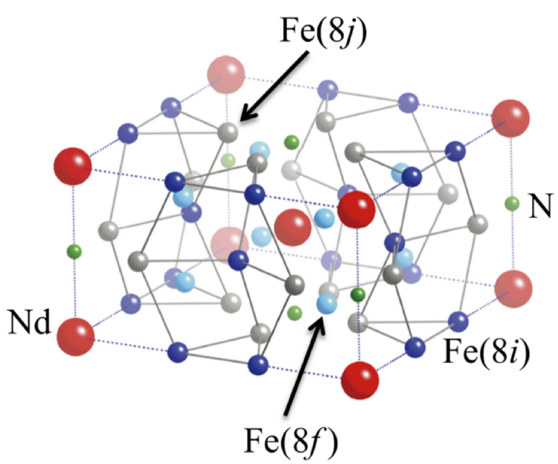

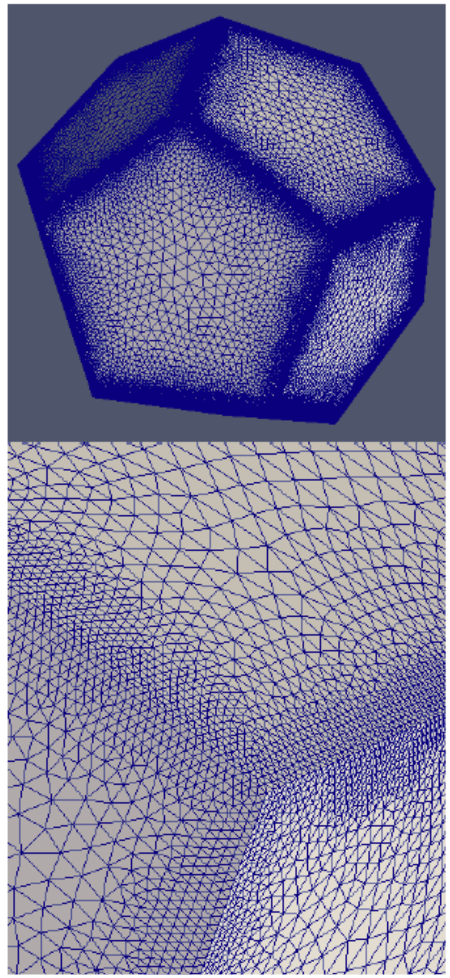

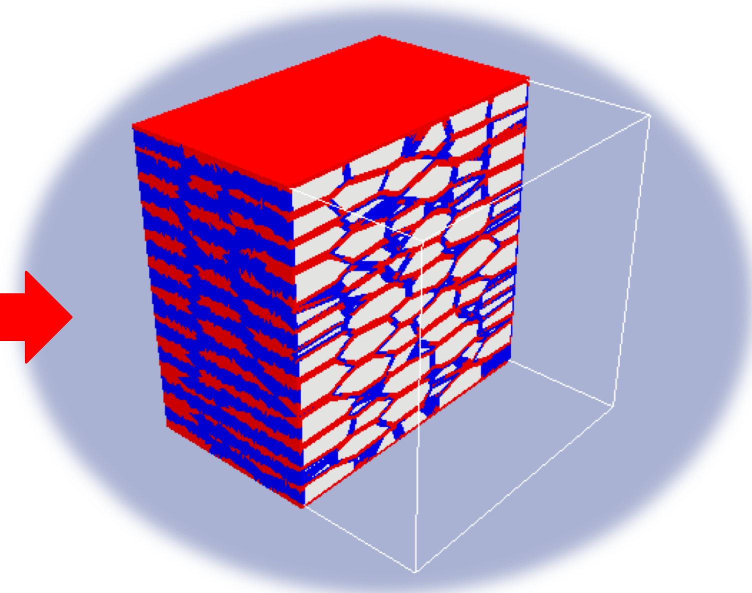

ab initio description of Nd2Fe14B

finite element modeling of grain

coarser finite element modeling of assembly of grains

Renormalization/Scaling theory of Micromagnetics

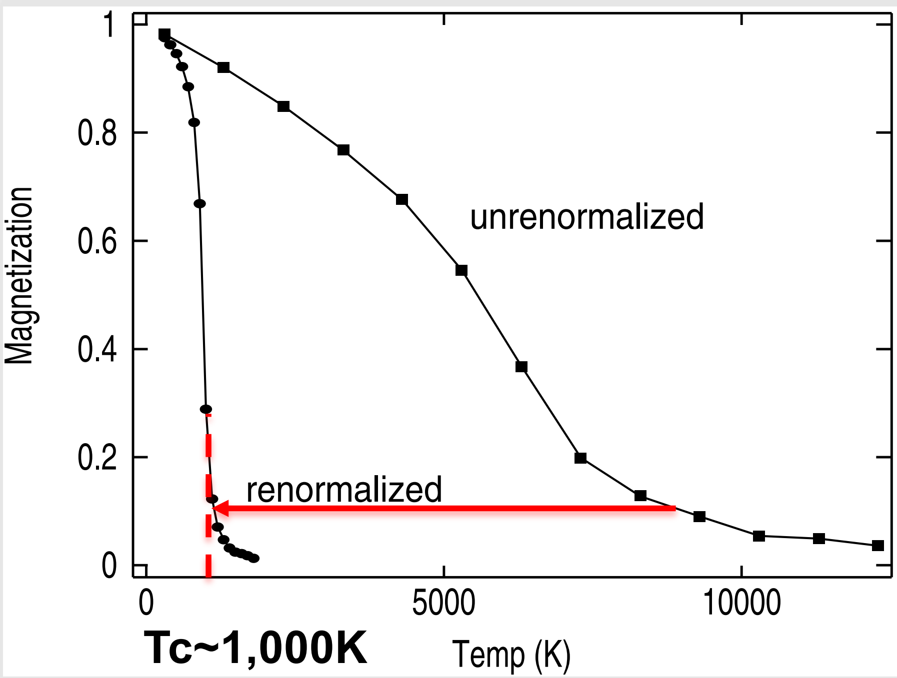

Renormalized FEM: Tc becomes realistic

Grinstein, Koch, PRL, 2003

Finite element micromagnetics (FEM) gets Tc very wrong for classes of materials, such as permalloy.

Reason: FEM parameters are taken from microscopic/macroscopic values and only trivially rescaled to *L*, the cell size of FEM

Idea: renormalize the FEM parameters of cells with size *L* also with fluctuations of wavelengths smaller than *L*: "integrate out spin fluctuations to length *L*"

$$E(\{\vec{S}\}) = \frac{J}{2}\int d^d x (\nabla \hat{s}(\vec{x}))^2$$

$$\partial T / \partial l = -\epsilon T + a T^2$$

dimensional rescale **fluctuations**

Renormalization/Scaling theory of Micromagnetics

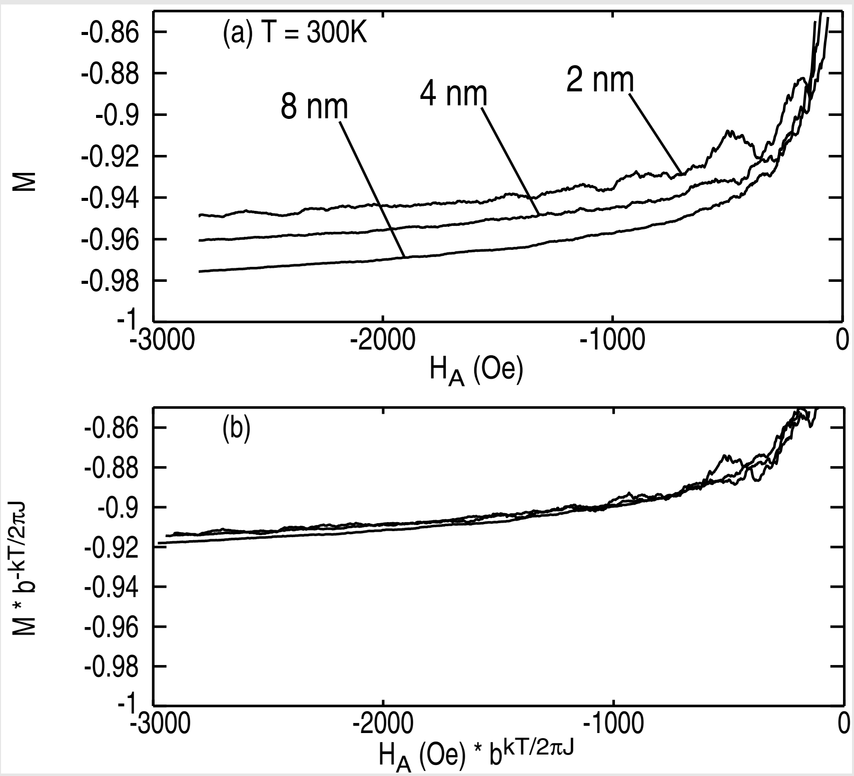

Grinstein, Koch, PRL, 2003

Renormalization at low T, in a limited magnetic field *h*:

$$dT(l)/dl = [-\epsilon + I(T(l), h(l))]T(l),$$

$$dh(l)/dl = 2h(l),$$

Upper Fig.: FEM simulation of magnetization with cell sizes *L*=2, 4, and 8nm gives size dependent results.

Lower Fig.: FEM with same *L*=2, 4, and 8 nm cell sizes but performed with renormalized parameters gives cell-size independent results.

Reversal, governed by domain wall-mediated nucleation, not captured well by spin waves

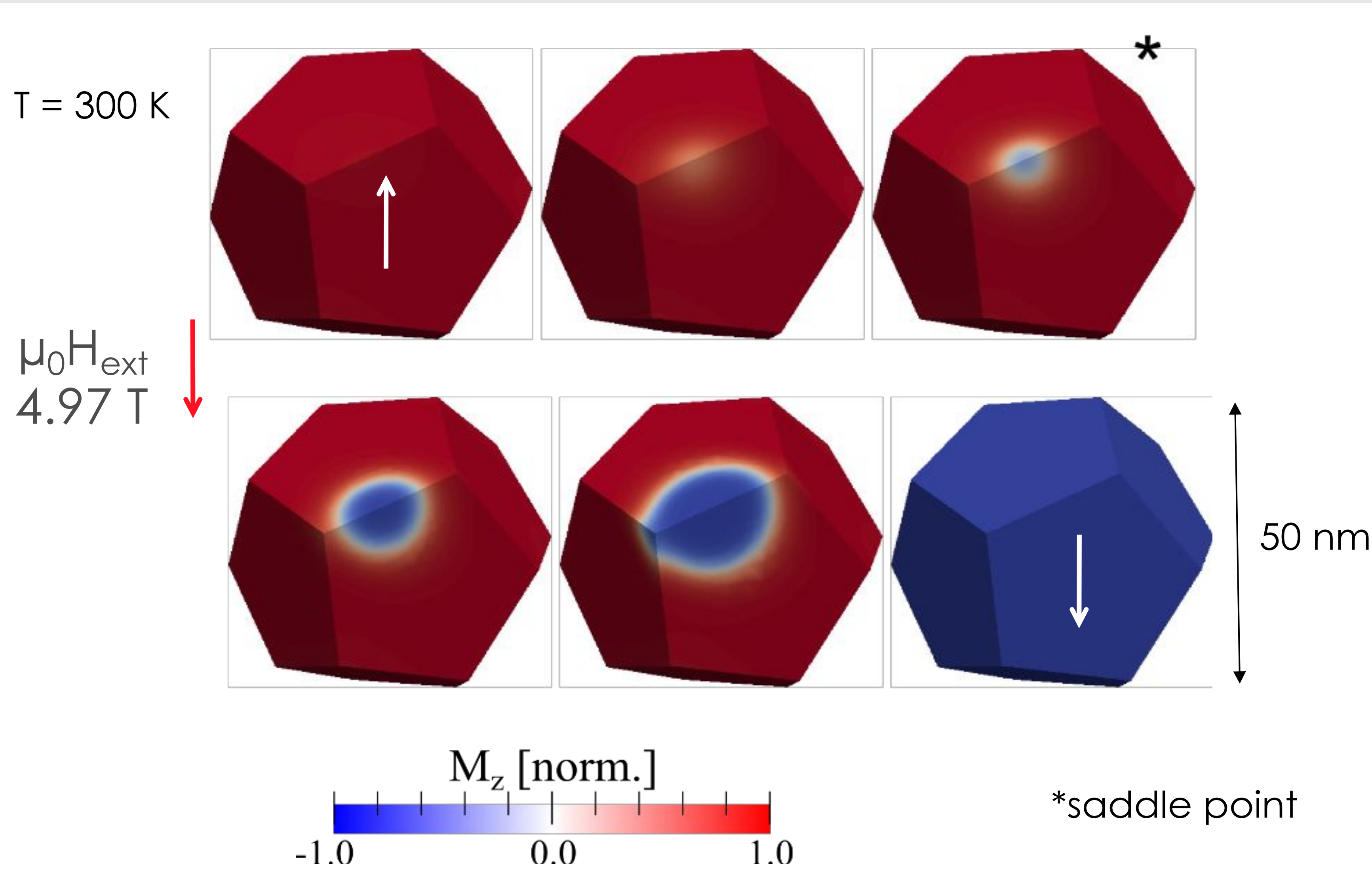

Reversal governed by fluctuations on multiple hierarchical scales

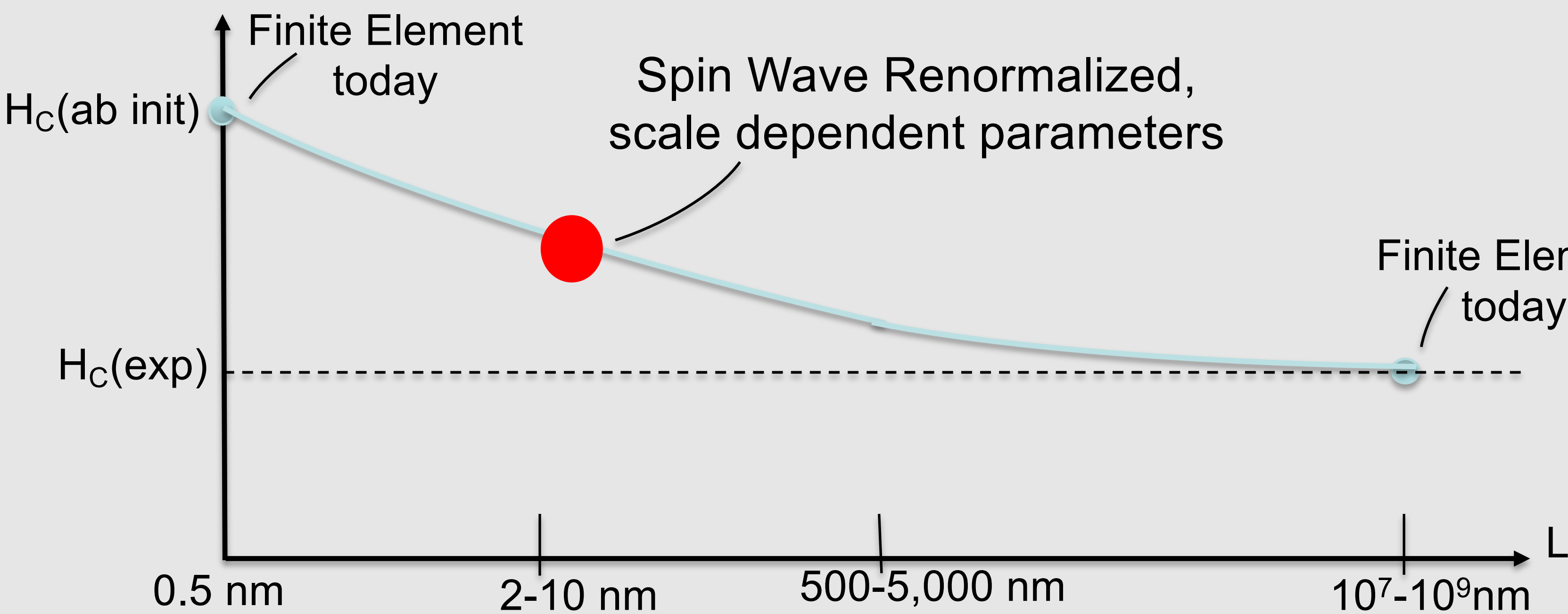

1. Atoms in unit cell	2. Spin waves in FE cells	3. Nucleation, reversal by domain walls	4. Average interactions, $H_K=\alpha K-N_{eff}M$	5. Macroscopic
Ab initio	*Analytic/RG*	*Finite Element*	*Mean field*	***Experiments***

Spin-Wave Renormalization of Finite Element Cell Parameters: $Nd_2Fe_{14}B$

$$\frac{M(L)}{M(exp)} = 1 + \frac{2\mu_B}{M(exp)} \frac{V}{(2\pi)^3} \iiint_{-\frac{\pi}{L}}^{\frac{\pi}{L}} dk \left[exp\left(\frac{E(k)}{kT}\right) - 1 \right]^{-1}$$

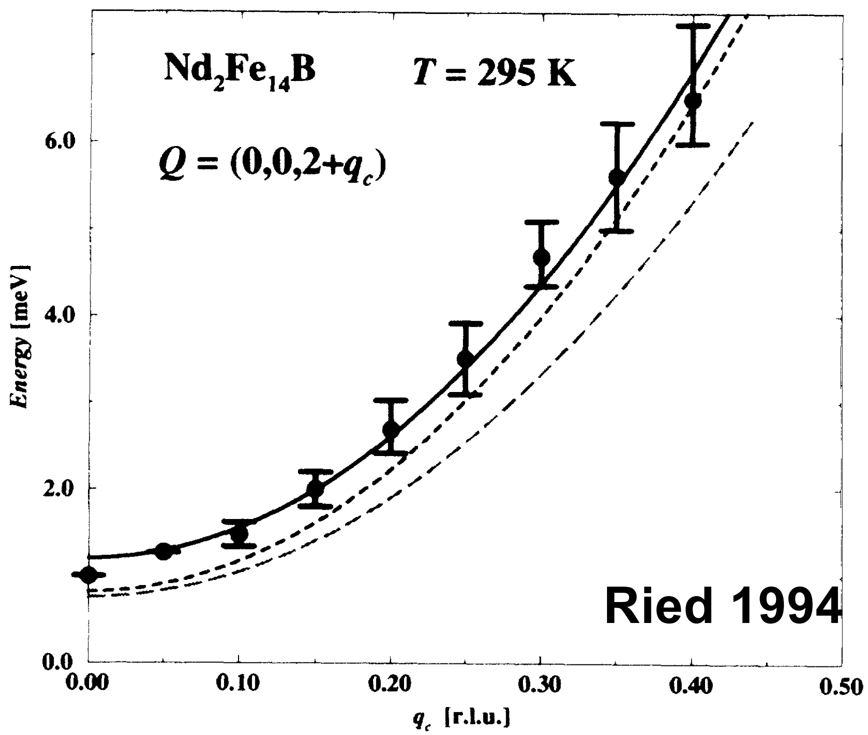

Ried 1994

$$E^{-}(\boldsymbol{q}) = 0.76 \text{ meV} + 107.3 \text{ meV Å}^2 q^2$$

T(K)	300K	450K
μ_0Ms(T)	1.61	1.29
A(pJ/m)	7.7	4.9
K (MJ/m^3)	4.3	2.9

Durst 1986

Spin Wave Renormalization induces 10-20% scale-dependent renormalization of parameters

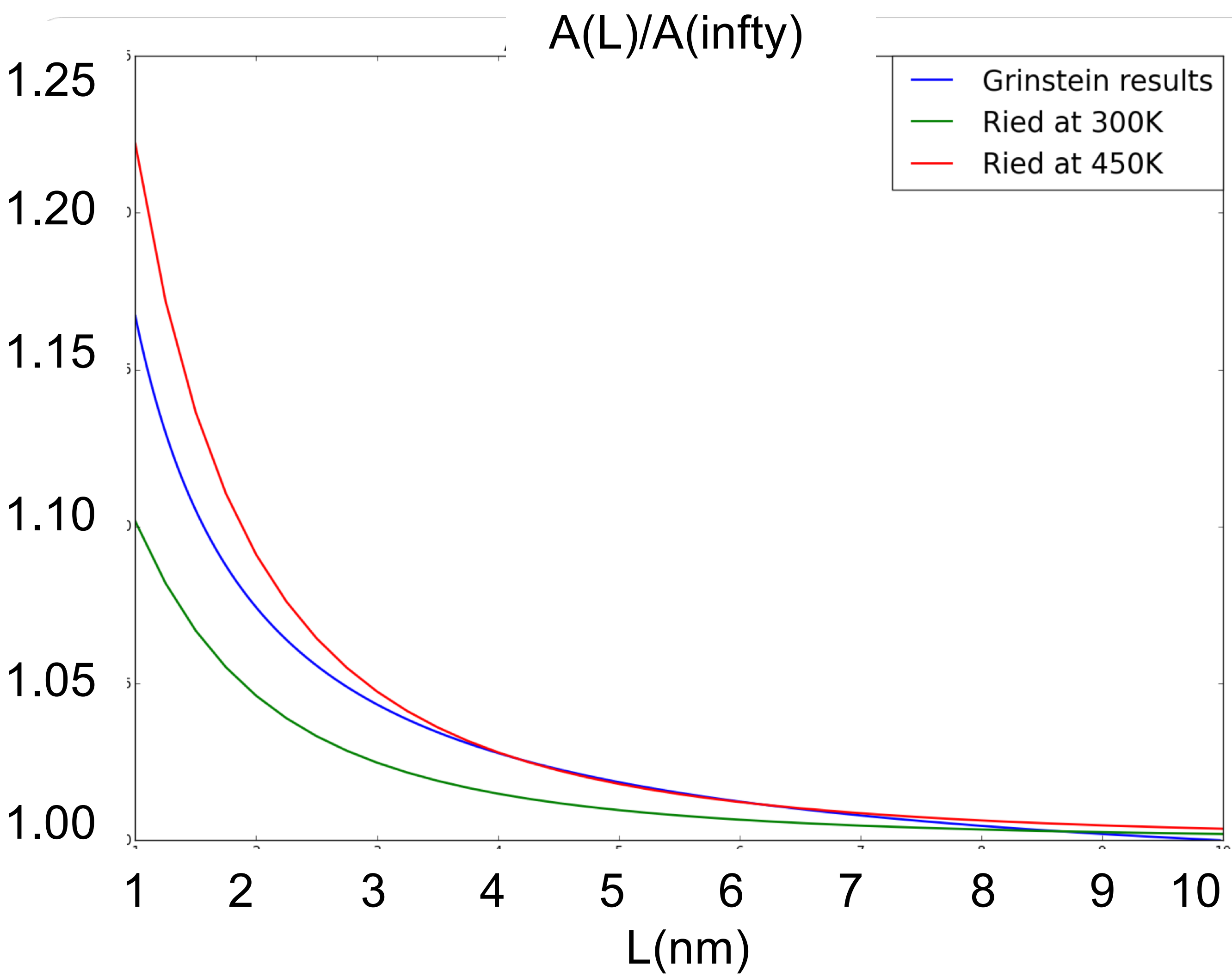

10-20% renormalization of ab initio parameters from L= 0.5 nm to 2 nm.

Hierarchical nanostructure, developed for Toyota

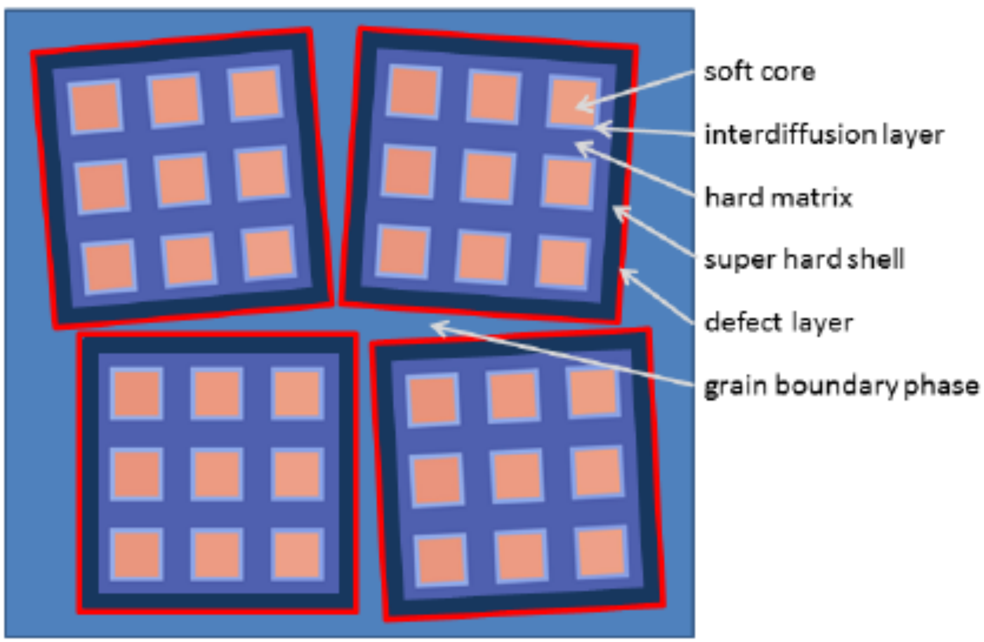

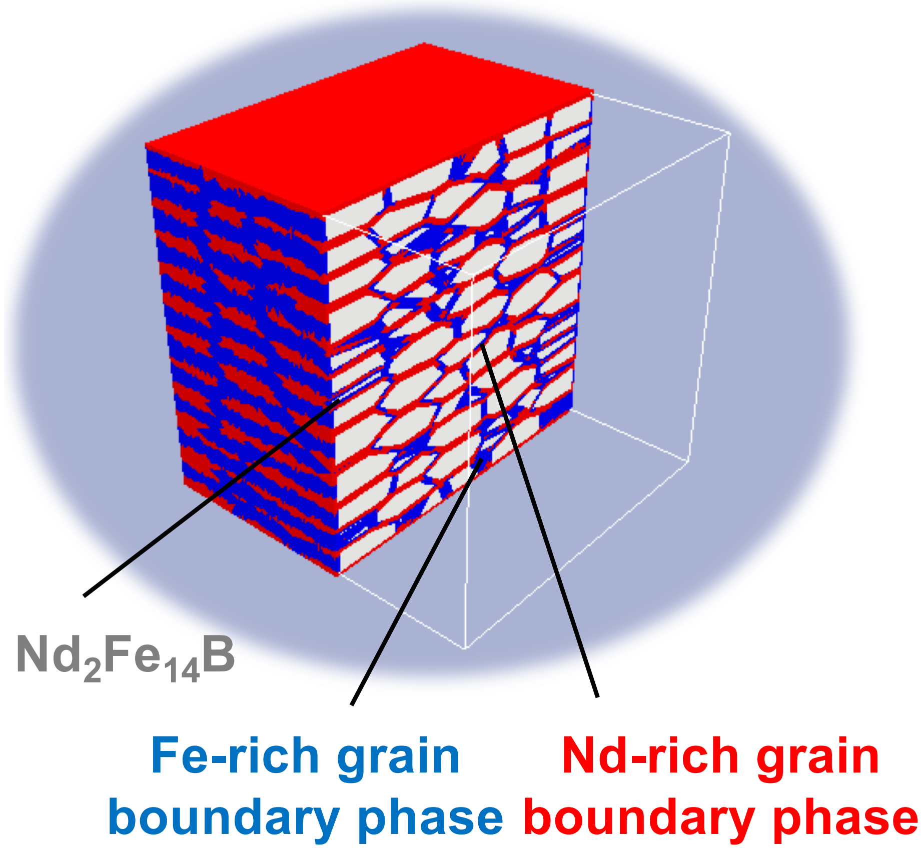

Our magnet is in the Toyota Prius

Scaling-correction
to coercive field

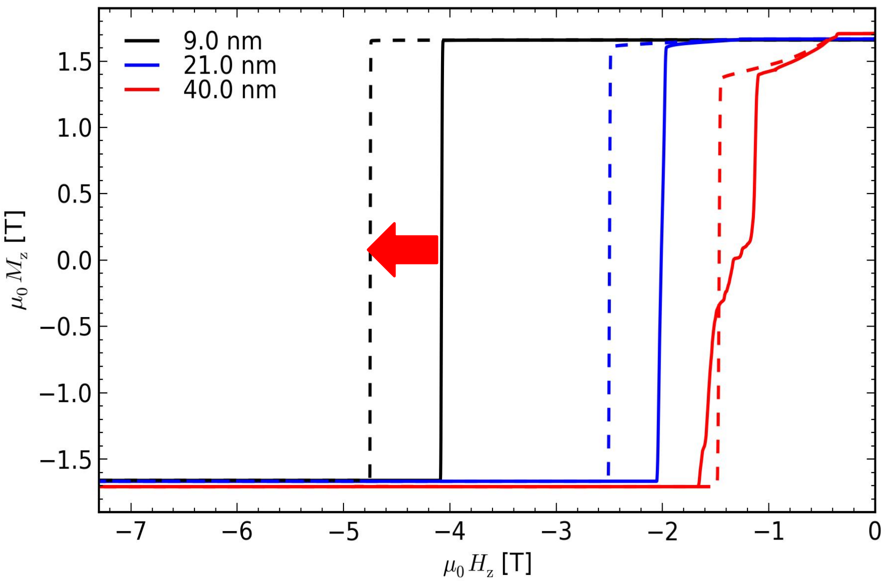

New Toyota magnet cuts dependence on key rare earth metal for EV motors

Reuters Staff

Reuters Feb. 20, 2018

(This February 20 story corrects paragraph 2 to say neodymium is used in permanent magnets, not batteries)

FILE PHOTO: A Toyota Prius (R) and a Prius V are displayed at the North American International Auto Show in Detroit, January 12, 2016. REUTERS/Mark Blinch/File Photo

5. Femtosecond lasers, developed by Mourou and Strickland, awarded Nobel in 2018

U.S. Patent Aug. 12, 1997 Sheet 2 of 10 5,656,186

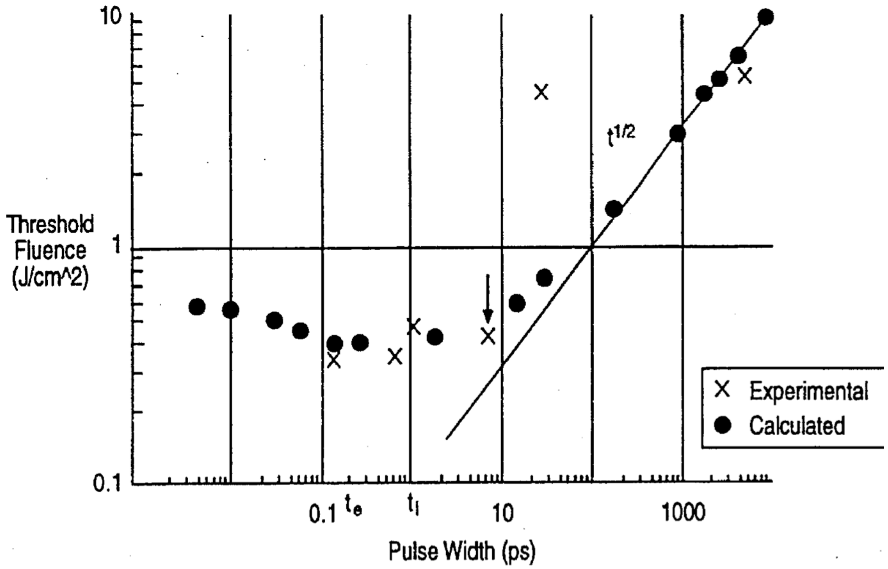

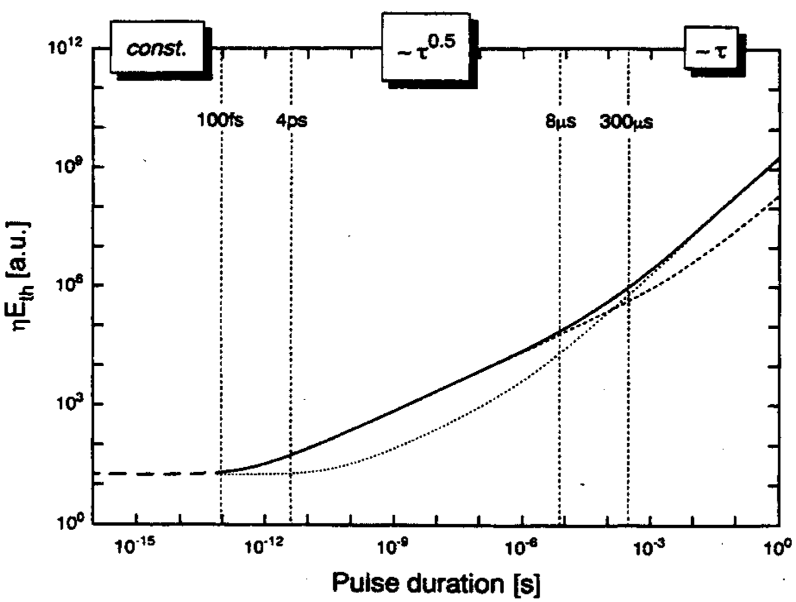

Figure 1 – Schematic processing comparison of microsecond to femtosecond lasers

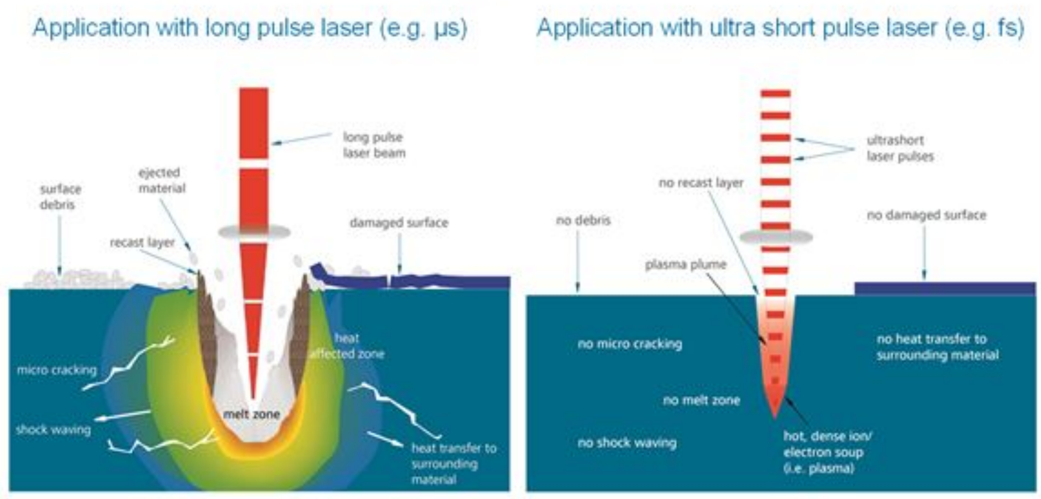

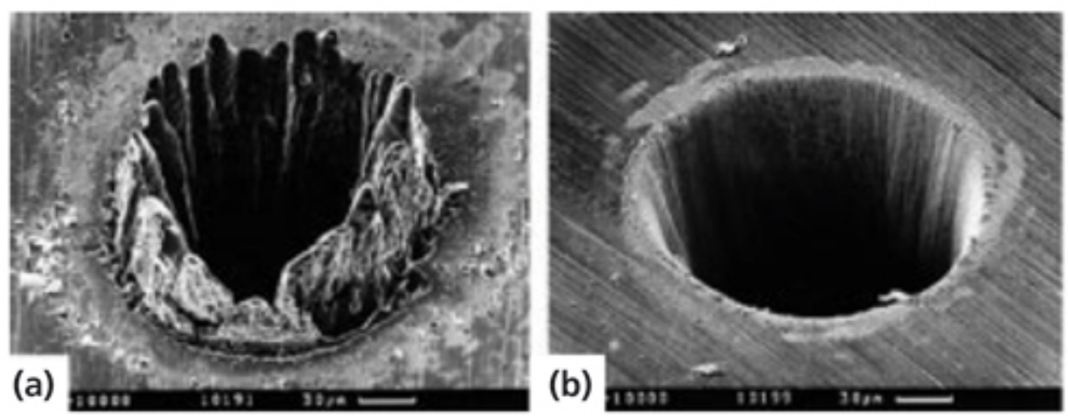

Chirped Pulse Amplification

Gerard Mourou
Donna Strickland

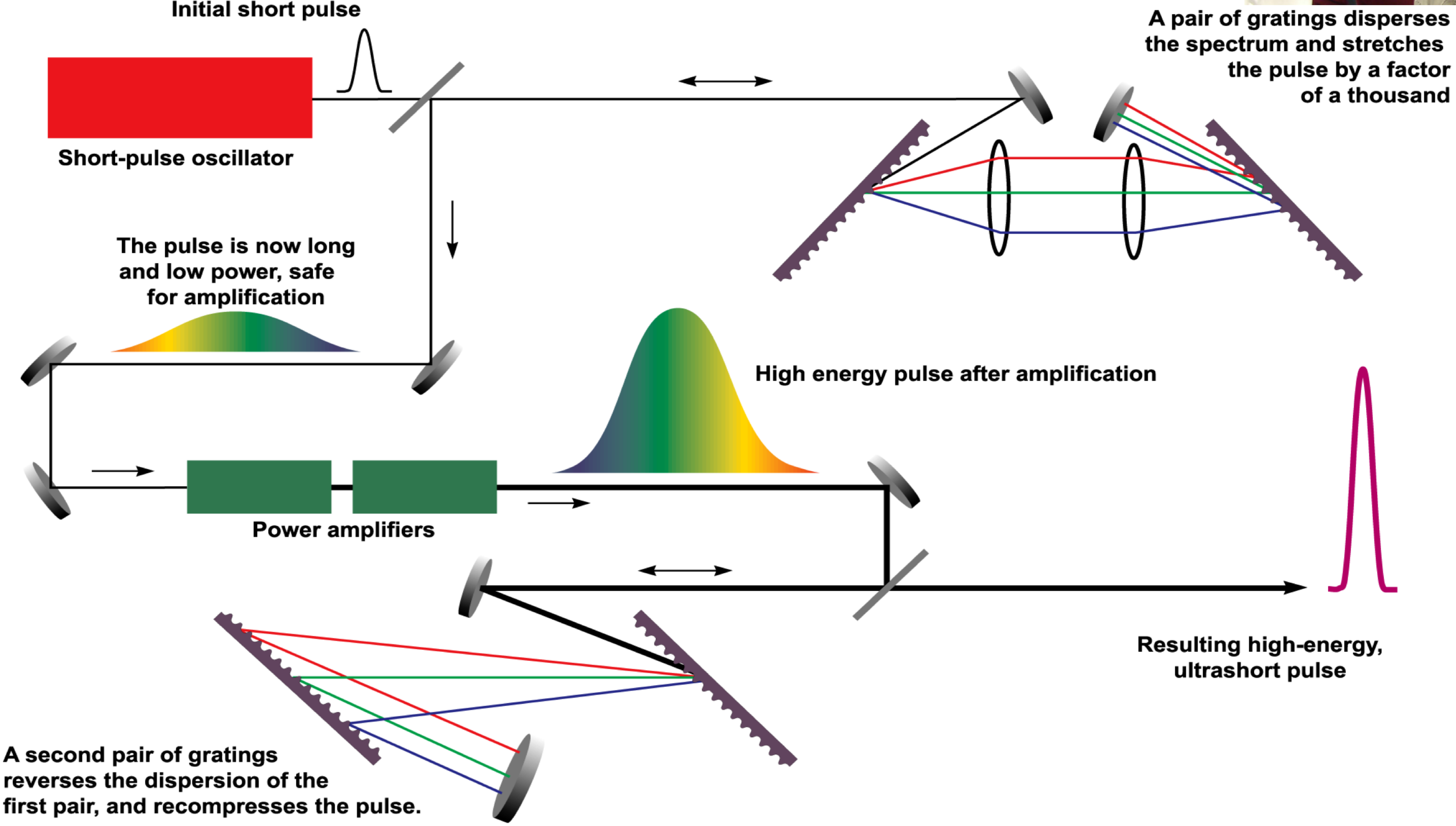

High precision medical imaging also needed: Test of relativity provides key

Imaging transparent tissue is big challenge for using femto lasers for eye surgery

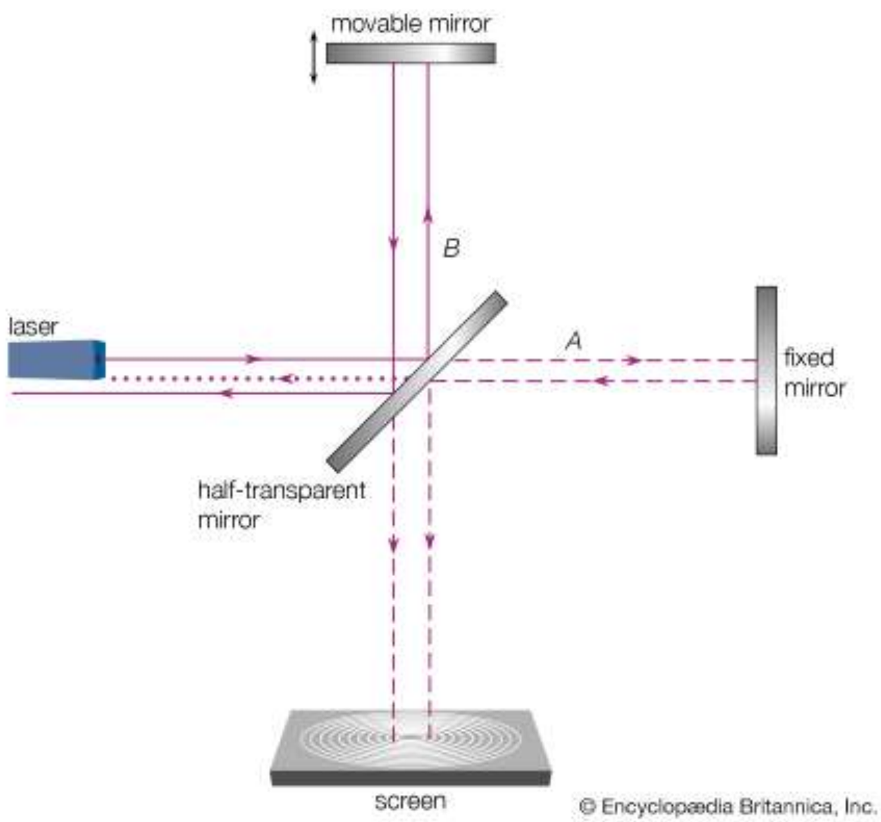

Michelson Morley interferometer, to test aether, leading to the Theory of Special Relativity (1887)

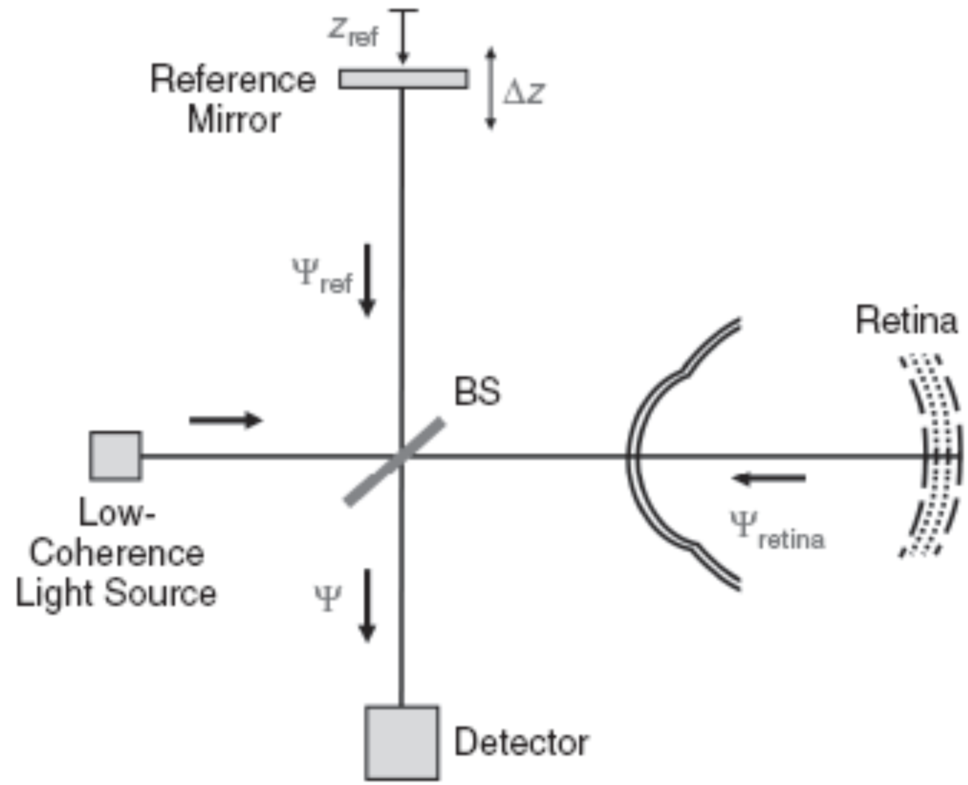

Optical Coherence Tomography (OCT), to provide in-depth images of transparent eye tissue (1987-1991)

Nobel winning femtosecond lasers restored the vision of more than a million patients

Femtosecond laser for precision cutting +
OCT for unprecedented imaging: the LenSx laser

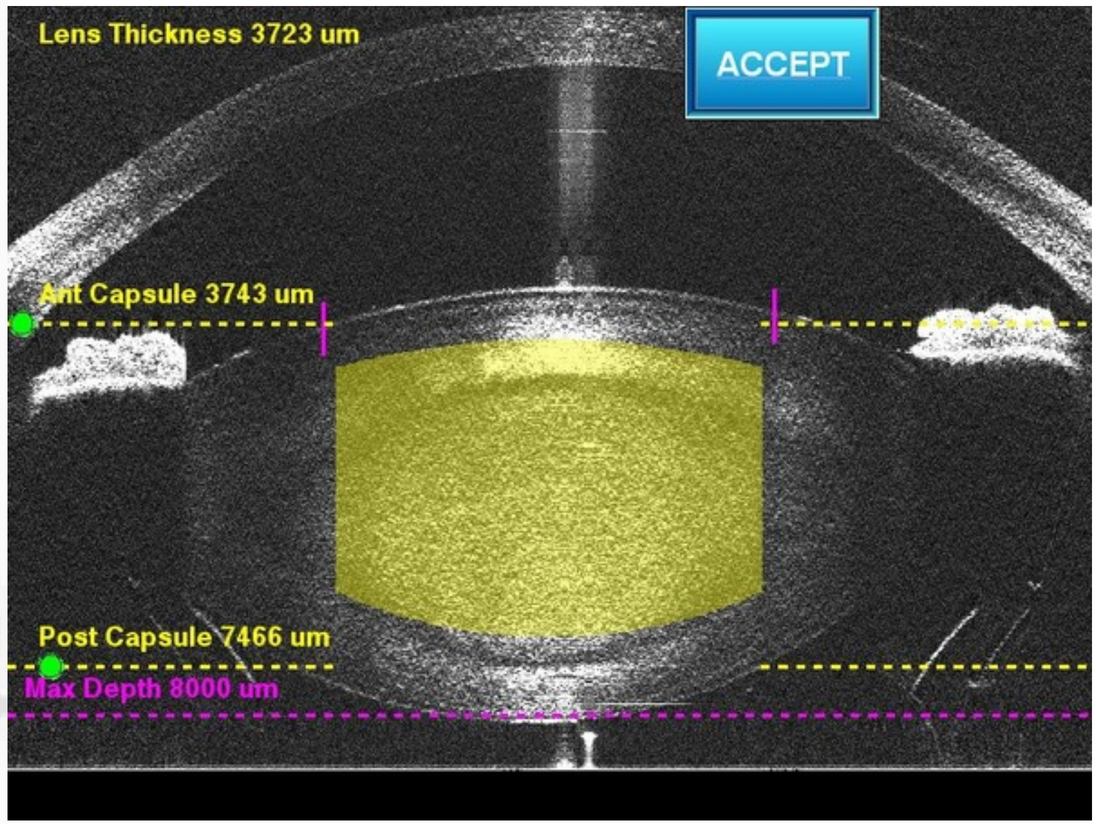

The LenSx femtosecond laser restored the vision of more than a million patients

Five pathways of basic science tools making direct impact in renewable energy and medicine

1. Strongly interacting electrons in perovskites	Boosting efficiency of energy conversion in solar cells
2. Metal-Insulator Transition	Improving charge extraction in solar cells
3. Quantum glassy dynamics	Mitigating performance degradation of world record holder Si solar cells
4. Renormalization group and scaling	Developing better magnets for the electromotor of the Toyota Prius
5. Test of Relativity + Nobel-winning femtosecond lasers	Creating LASIK and laser cataract eye surgery